

Supporting Information: Confined electroconvective vortices at structured ion exchange membranes

Joeri de Valença ^{a,b,†}, Morten Jøgi ^b, R. Martijn Wagterveld ^b, Elif Karatay ^c,
Jeffery A. Wood ^a, and Rob G.H. Lammertink ^{a,**}

^a*Soft Matter, Fluidics and Interfaces Group, MESA⁺ Institute of Nanotechnology,
University of Twente, 7500AE, Enschede, The Netherlands;*

^b*Wetsus, European Centre of Excellence for Sustainable Water Technology, Oostergoweg 9,
8911MA, Leeuwarden, The Netherlands;*

^c*Department of Mechanical Engineering, Stanford University, Stanford, California 94305,
USA*

E-mail: r.g.h.lammertink@utwente.nl

Conductivity calibration curve

The conductivity has an almost linear relation with the electrolyte concentration. Figure S1 shows a calibration curve of conductivity of a CuSO₄ electrolyte. The resistance of the electrolyte is inversely proportional to the concentration:

$$\sigma = \frac{A}{R \cdot l} \sim c \quad (\text{S1})$$

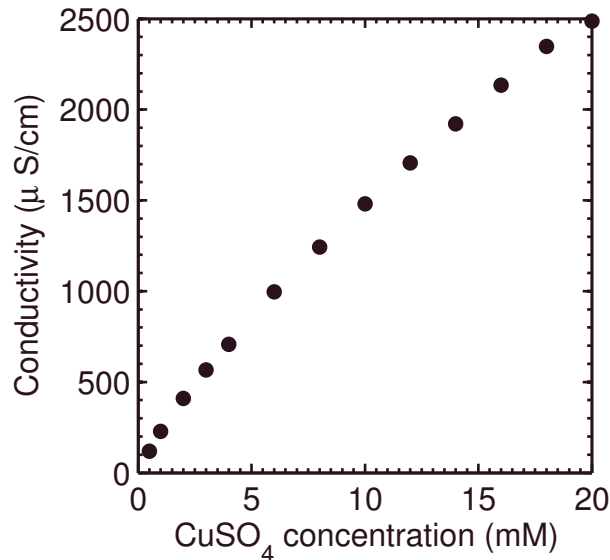


Figure S1: Calibration curve of CuSO_4 concentration vs conductivity.

where R is the resistance between two surfaces, l is the length between the surfaces, A is the area of the surfaces, σ is the conductivity of the electrolyte and c the ionic concentration in the electrolyte. A thin layer with low concentration can dominate the overall resistance. This is the reason the mixing layer dominates the overall overlimiting resistance. This also means that relating the conductivity in the mixing layer to the average concentration in the mixing layer underestimates the value. Although the mixing layer has a lower gradient than the diffusion layer, still a gradient occurs. Again the layer with lower concentration dominates the resistance.

Reproducibility of measurements with same membrane

To achieve a statistically significant result, multiple measurements were conducted with the same membrane. Each measurement is done with a new homogeneous solution, which meant the cell had to be disassembled and assembled between measurements. This was done with great care, but degradation of the membrane over time was observed nonetheless. Figure S2

shows the change in the surface of the 200 μm membrane. The overlimiting current through to wrinkled surface of the seventh measurements has a higher resistance and a smaller mixing layer, resulting in a low conductivity, see the table below.

Table S1: Saturation Resistance, Mixing Layer Length and Conductivity for Different Measurements

| number | R_{sat} (k Ω) | L_{mix} (μm) | σ ($\mu\text{S}/\text{cm}$) |
|--------|--------------------------------|------------------------------------|--------------------------------------|
| 1 | 6.6 | 410 | 62 |
| 2 | 6.4 | 373 | 58 |
| 5 | 8.3 | 370 | 44 |
| 7 | 12.6 | 327 | 26 |

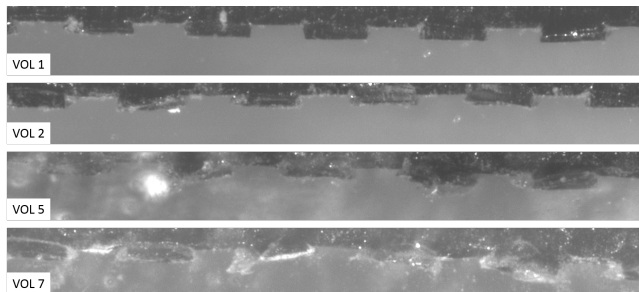


Figure S2: Front view of the same membrane with 200 μm structures in the test cell. After multiple usages the membrane surface becomes rougher

The seventh run of this experiment was excluded since the structure does not represent the periodic membrane as seen in the first measurement. The resistance and mixing layer thickness data confirm that it is essential to have a periodic surface structure to get periodic and confined vortices. Measurement number five was included in the analysis. The structure is not perfect and it has a higher resistance, but the mixing layer thickness was similar.

Simulation of Transient Vortex

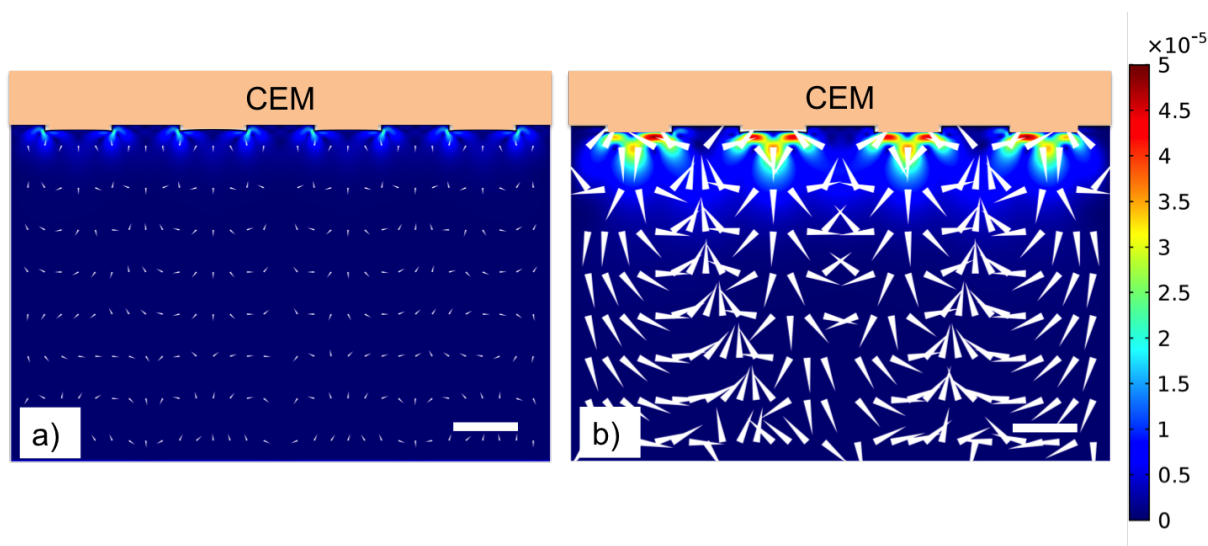


Figure S3: (a) Velocity Profiles at Dimensionless time $\simeq 0.01$ and (b) Dimensionless time $\simeq 0.1$. The scalebar represents $400 \mu\text{m}$, velocities are shown in m/s

The simulations were solved in a transient manner, Figure 8 in the main text shows the velocity profile after achieving steady-state and shows the values at two time-snap shows to illustrate the growth of vortices.

Supplemental movies

Six supporting movies are provided. The first three movies show the electroconvective motion near three different structured membranes by looking at the particle pathlines. The fourth movie is made from raw images to show the inner and outer vortices at the membrane structures. The fifth movie displays the derived vector fields. The sixth movie presents the change in lifetime due to the concentration polarization. All measurements have initially the same salt concentration (10 mM CuSO_4) and the same applied voltage (1 V) is applied.

The first three supporting movies are made from particle image stacks. Each image is an overlay of 100 particle images (ImageJ, Z project, max intensity), displaying the particle pathlines over 10 s (10 fps). In time the electroconvective layer grows, the corresponding

current density drops and the resistance increases (see Figure 3a main paper). At the flat membrane (movie 1) the electroconvective vortices start randomly. The mixing layer grows till a saturated size while the individual vortices move randomly around. At the 100 μm structured membrane (movie 2) the vortices motion follows the periodicity of the membrane structures. When the vortices grow they become too big to follow the periodicity of the membrane. At the 400 μm structured membrane (movie 3) the vortex onset also follows the periodicity of the membrane, therefore displaying less vortices than at the 100 μm membrane. When the vortex mixing layer reaches the saturated size (≈ 0.5 mm) the vortices periodicity still follows the membrane structure, which we call confined vortices.

Movie 4 shows the particle images of the vortex onset near the 100 μm structured membrane. From the electrical data the transition times are extracted as $\tau_C = 44$ s and $\tau_{EC} = 55$ s. From $t = 60$ s the distinction between the inner and outer vortices is visible. The inner vortices cannot grow since they are confined by the membrane gap. An extra image is supplied which shows the membrane interface by using front illumination.

Movie 5 displays the the flow fields (every 5 s) obtained with PIV analysis from the particle recordings at a 400 μm structured membrane. Each vector field is calculated by taking the sliding average of five consecutive vector fields with (each $dt = 0.1$ s). The length of the vectors represents the velocity size and direction. The background color represents the calculated vorticity.

Movie 6 is a visualization of the concentration polarization using fluorescence lifetime imaging microscopy (FLIM). The pixel color represents the calculated lifetime of the fluorescent Alexa 488 dye. The lifetime of the dye depends on the ionic strength with known calibration curve related to the CuSO_4 concentration, see Figure S4. Each frame displays the average calculated lifetime over three measurements of each 5 s. The periodicity of the membrane structures (800 μm) is visible in fluid as the lifetime in front of the extrusion is lower than in front of the gap. This indicated a lower concentration in front of the extru-

sion and higher in front of the gap. This observation agrees with the observation that the depleted electrolyte moves away from the membrane in front of the extrusion. After 1000 s the electric forcing stops as well as the electroconvection. In time the concentration gradient diminishes due to diffusion.

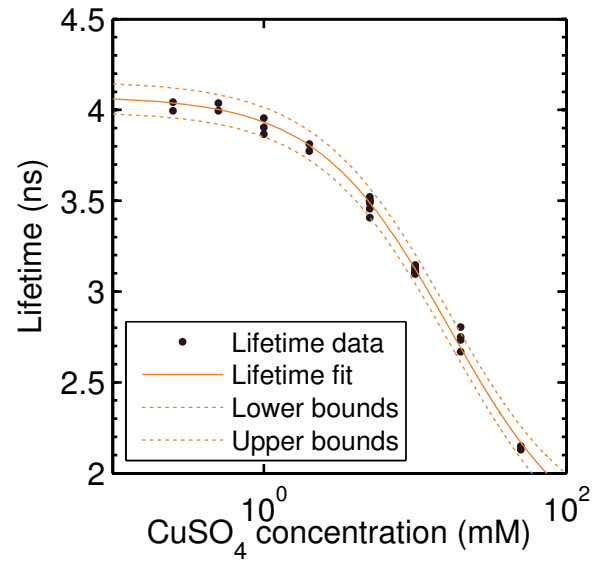


Figure S4: Lifetime vs concentration calibration curve on semi-log scale.